

Measurement of the total cross section at 8 TeV and the inelastic cross section at 13 TeV at the LHC with the ATLAS detector

Hasko Stenzel
on behalf of the ATLAS Collaboration¹

¹*II Physikalisches Institut, Justus-Liebig University Giessen, Heinrich-Buff Ring 16, D-35392 Giessen, Germany.*

Hasko.Stenzel@cern.ch

Abstract. New measurements from ATLAS at the LHC are presented on the total cross section at $\sqrt{s} = 8$ TeV from elastic scattering using the ALFA sub-detector and on the inelastic cross section at $\sqrt{s} = 13$ TeV using the MBTS sub-detector.

Introduction

The rise of the total proton-proton (pp) cross section with center-of-mass energy \sqrt{s} , predicted by Heisenberg [1] and observed at the CERN Intersecting Storage Rings [2, 3], probes the non-perturbative regime of quantum chromodynamics. Arguments based on unitarity, analyticity, and factorization imply an upper bound on the high-energy behaviour of total hadronic cross sections that prevents them from rising more rapidly than $\ln^2(s)$ [4, 5, 6]. The rise of the total and inelastic cross section in the energy range of the LHC is further confirmed by two new measurements from the ATLAS collaboration. At the highest centre-of-mass energy of 13 TeV a first measurement of the inelastic cross section is performed [7] and at 8 TeV the total cross section is determined [8].

The inelastic cross section at $\sqrt{s} = 13$ TeV

The measurement of the inelastic yield is based on the counting of hits in the Minimum Bias Trigger Scintillator (MBTS), which is a plastic scintillator located in front of the end-cap calorimeters at a distance of 3.6 m from the interaction point in the forward region ($2.07 < |\eta| < 3.86$). The counters are sensitive to diffractive dissociation processes with masses of the diffractive system $M_X > 13$ GeV, or equivalently, $\xi = M_X^2/s > 10^{-6}$. Thus the inelastic cross section is primarily reported inside this fiducial volume corresponding to $\xi > 10^{-6}$, and then extrapolated to full phase space with the help of models for the total inelastic cross section. Data were collected in a special run at low luminosity and low pile-up in which an integrated luminosity of about $60 \mu\text{b}^{-1}$ was accumulated. In order to select inelastic events nominally two hits in the MBTS are requested in any of the counters, additionally a single-diffraction enhanced sample is selected by requiring two counters with hits on the same side with a veto at the other side. The ratio of the number of events with a single-side tag and the number of inclusive events, R_{SS} , is used to constrain in the simulation the relative contributions of single- and double-diffraction ($\sigma_{\text{SD}} + \sigma_{\text{DD}}$) to the inelastic cross section, $f_{\text{D}} = (\sigma_{\text{SD}} + \sigma_{\text{DD}})/\sigma_{\text{inel}}$, using a procedure developed in Ref. [9]. The resulting predictions for the MBTS hit distribution from different models, all tuned to reproduce the measured value $R_{\text{SS}} = 10.4 \pm 0.4\%$, are shown in Fig. 1. The fiducial cross section is determined by

$$\sigma_{\text{inel}}^{\text{fid}}(\xi > 10^{-6}) = \frac{N - N_{\text{BG}}}{\epsilon_{\text{trig}} \times \mathcal{L}} \times \frac{1 - f_{\xi < 10^{-6}}}{\epsilon_{\text{sel}}}, \quad (1)$$

where N is the number of observed events passing the inclusive selection, N_{BG} is the number of background events, ϵ_{trig} and ϵ_{sel} are factors accounting for the trigger and event selection efficiencies, $1 - f_{\xi < 10^{-6}}$ accounts for the migration

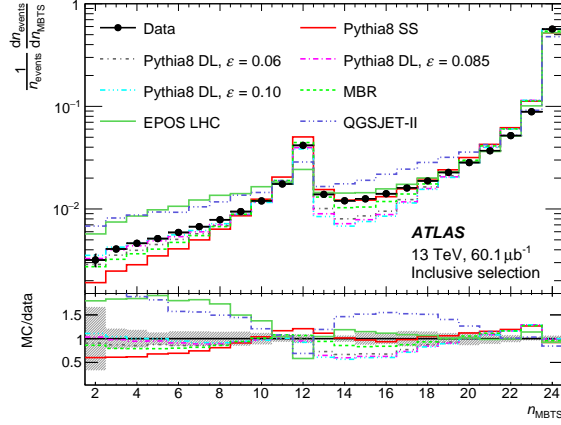


FIGURE 1. The background-subtracted distribution of the number of MBTS counters above threshold in data and MC simulation for the inclusive selection. The MC models are defined in Ref. [7] and their ratio to the data is also shown. The experimental uncertainty is shown as a shaded band around the data points. The models shown here use the f_D value determined from the R_{SS} measurement. Figure from Ref.[7].

of events with $\xi < 10^{-6}$ into the fiducial region, and \mathcal{L} is the integrated luminosity of the sample. The measured fiducial cross section is determined to be $\sigma_{\text{inel}}^{\text{fid}} = 68.1 \pm 0.6$ (exp.) ± 1.3 (lum.) mb. The extrapolation to σ_{inel} uses constraints from previous ATLAS measurements to minimize the model dependence of the component that falls outside the fiducial region. σ_{inel} can be written as

$$\sigma_{\text{inel}} = \sigma_{\text{inel}}^{\text{fid}} + \sigma^{7 \text{ TeV}}(\xi < 5 \times 10^{-6}) \times \frac{\sigma^{\text{MC}}(\xi < 10^{-6})}{\sigma^{7 \text{ TeV, MC}}(\xi < 5 \times 10^{-6})}. \quad (2)$$

The term $\sigma^{7 \text{ TeV}}(\xi < 5 \times 10^{-6}) = \sigma_{\text{inel}}^{7 \text{ TeV}} - \sigma^{7 \text{ TeV}}(\xi > 5 \times 10^{-6}) = 9.9 \pm 2.4$ mb is the difference between σ_{inel} measured at 7 TeV using the ALFA detector [10], $\sigma_{\text{inel}}^{7 \text{ TeV}}$, and σ_{inel} measured at 7 TeV for $\xi > 5 \times 10^{-6}$ using the MBTS [9]. This and other inelastic cross-section measurements are compared to several Monte Carlo models in

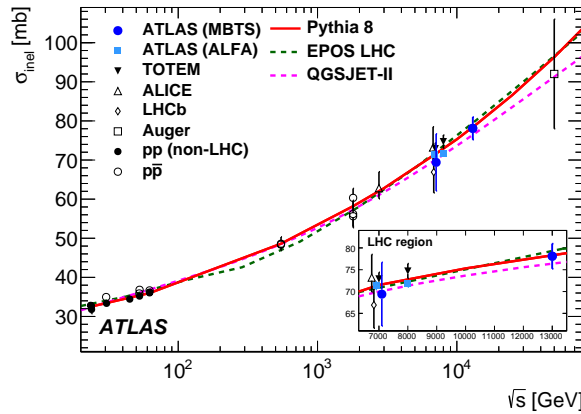


FIGURE 2. The inelastic proton-proton cross section versus \sqrt{s} . Measurements from other hadron collider experiments and the Pierre Auger experiment are also shown. The measurements are compared to the PYTHIA8, Epos LHC and QGSJet-II MC generator predictions. Figure from Ref.[7].

Figure 2. The measured value for σ_{inel} is

$$\sigma_{\text{inel}} = 78.1 \pm 0.6 \text{ (exp.)} \pm 1.3 \text{ (lum.)} \pm 2.6 \text{ (extr.) mb.}$$

The total cross section at $\sqrt{s} = 8$ TeV

The total cross section is determined from elastic scattering data collected in a special run with $\beta^* = 90$ m using the ALFA Roman Pot sub-detector [11]. The optical theorem is exploited to extract the total cross section σ_{tot} from a fit to the differential elastic cross section according to

$$\sigma_{\text{tot}}^2 = \frac{16\pi(\hbar c)^2}{1 + \rho^2} \left. \frac{d\sigma_{\text{el}}}{dt} \right|_{t \rightarrow 0}, \quad (3)$$

where ρ represents a small correction arising from the ratio of the real to the imaginary part of the elastic-scattering amplitude in the forward direction. Elastic events are selected with reconstructed tracks in four ALFA detectors with a trigger condition imposing a coincidence between the left and right arm of the set-up [8]. Further cuts are imposed on the acollinearity of the events in order to reject background. The residual background contamination is determined from the data and subtracted. The resulting sample consisting about 3.8 M events. For each event the t -value is calculated according to $-t = (\theta^* \times p)^2$, where p represents the nominal beam momentum and the scattering angle is calculated from the proton trajectories and beam optics parameters. The t -spectrum is unfolded for detector resolution and beam divergence effects and corrected for acceptance losses. The acceptance and unfolding corrections are calculated from a simulation tuned to account for the measured beam emittance and detector resolution [8]. The rate of elastic events is further corrected for reconstruction inefficiencies occurring in events developing hadronic showers according to a data-driven procedure [8]. Finally the integrated luminosity for this run is determined to be $L_{\text{int}} = 496.3 \pm 0.3$ (stat.) ± 7.3 (syst.) μb^{-1} , where the systematic uncertainty of 1.5% is dominated by the absolute luminosity scale calibration [12]. The differential elastic cross section in a given bin t_i is calculated from the following formula:

$$\frac{d\sigma_{\text{el}}}{dt_i} = \frac{1}{\Delta t_i} \times \frac{\mathcal{M}^{-1}[N_i - B_i]}{A_i \times \epsilon^{\text{reco}} \times \epsilon^{\text{trig}} \times \epsilon^{\text{DAQ}} \times L_{\text{int}}}, \quad (4)$$

where Δt_i is the width of the bins in t , \mathcal{M}^{-1} symbolizes the unfolding procedure applied to the background-subtracted number of events $N_i - B_i$, A_i is the acceptance, ϵ^{reco} is the event reconstruction efficiency, ϵ^{trig} is the trigger efficiency, ϵ^{DAQ} is the dead-time correction and L_{int} is the integrated luminosity. From a fit to the differential elastic cross section

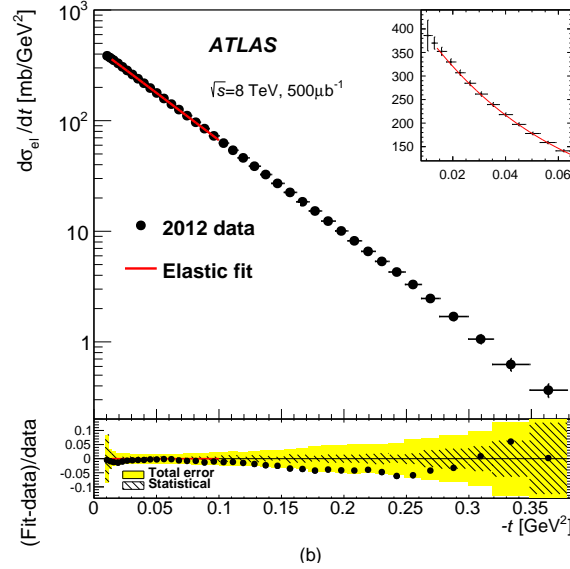


FIGURE 3. The fit of the theoretical prediction to the differential elastic cross section with σ_{tot} and B as free parameters. In the lower plot the points represent the relative difference between fit and data, the yellow area represents the total experimental uncertainty and the hatched area the statistical component. The red line indicates the fit range; the fit result is extrapolated in the lower plot outside the fit range. The upper right insert shows a zoom of the data and fit at small t . Figure from Ref.[8].

shown in Fig. 3, which included both statistical and experimental systematic uncertainties [8], the value of σ_{tot} and of

the nuclear slope parameter B are extracted. The fit yields for the total cross section at $\sqrt{s} = 8$ TeV

$$\sigma_{\text{tot}}(pp \rightarrow X) = 96.07 \pm 0.18 \text{ (stat.)} \pm 0.85 \text{ (exp.)} \pm 0.31 \text{ (extr.) mb} ,$$

where the first error is statistical, the second accounts for all experimental systematic uncertainties and the last is related to uncertainties in the extrapolation $t \rightarrow 0$. In addition, the slope of the elastic differential cross section at small t is determined to be $B = 19.74 \pm 0.05 \text{ (stat.)} \pm 0.23 \text{ (syst.) GeV}^{-2}$. The dominant contributions to the systematic uncertainty arise from the luminosity and from the beam energy. The measurement of ATLAS is compared to measurements at lower energy and to a global fit in Figure 4.

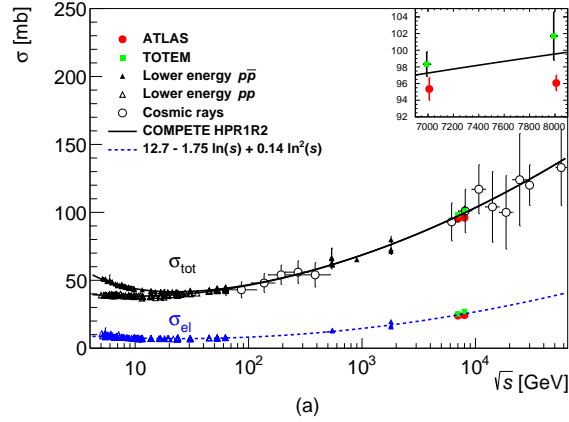


FIGURE 4. Comparison of total and elastic cross-section measurements presented here with other published measurements and model predictions as a function of the centre-of-mass energy. Figure from Ref.[8].

Conclusion

The ATLAS Collaboration has performed new measurements of the total cross section at $\sqrt{s} = 8$ TeV and of the inelastic cross section at $\sqrt{s} = 13$ TeV. The main results are:

$$\begin{aligned} \sigma_{\text{tot}}(8 \text{ TeV}) &= 96.07 \pm 0.18 \text{ (stat.)} \pm 0.85 \text{ (exp.)} \pm 0.31 \text{ (extr.) mb} , \\ \sigma_{\text{inel}}(13 \text{ TeV}) &= 78.1 \pm 0.6 \text{ (exp.)} \pm 1.3 \text{ (lum.)} \pm 2.6 \text{ (extr.) mb} . \end{aligned}$$

REFERENCES

- [1] W. Heisenberg, *Z. Phys.* **133**, 65–79 (1952).
- [2] S. R. Amendolia *et al.*, *Phys. Lett. B* **44**, p. 119 (1973).
- [3] U. Amaldi *et al.*, *Phys. Lett. B* **44**, p. 112 (1973).
- [4] M. Froissart, *Phys. Rev.* **123**, p. 1053 (1961).
- [5] A. Martin, *Nuovo Cim. A* **42**, p. 930 (1966).
- [6] A. Martin, *Phys. Rev. D* **80**, p. 065013 (2009), arXiv:0904.3724 [hep-ph] .
- [7] ATLAS Collaboration, *Phys. Rev. Lett.* **117**, p. 182002 (2016), arXiv:1606.02625 [hep-ex] .
- [8] ATLAS Collaboration, *Phys. Lett. B* **761**, p. 158 (2016), arXiv:1607.06605 [hep-ex] .
- [9] ATLAS Collaboration, *Nature Commun.* **2**, p. 463 (2011), arXiv:1104.0326 [hep-ex] .
- [10] ATLAS Collaboration, *Nucl. Phys. B* **889**, p. 486 (2014), arXiv:1408.5778 [hep-ex] .
- [11] S. Abdel Khalek *et al.*, (2016), arXiv:1609.00249 [physics.ins-det] .
- [12] ATLAS Collaboration, (2016), arXiv:1608.03953 [hep-ex] .